Comparison of a VLBI TRF Solution Based on Kalman Filtering and Recent ITRS Realizations

Benedikt Soja[1], Tobias Nilsson[1], Susanne Glaser[2], Kyriakos Balidakis[2], Maria Karbon[1], Robert Heinkelmann[1], Richard Gross[3], Harald Schuh[1,2]

Abstract Terrestrial reference frames (TRFs) of high quality are indispensable for many geoscientific and geodetic applications including very long baseline interferometry (VLBI) data analysis. While secular station coordinate changes, for instance due to tectonic plate motion, are well represented by a linear model, current accuracy requirements demand modeling of non-linear signals such as surface deformations due to mass loading or post-seismic deformations. In this paper, we portray a TRF solution solely based on VLBI data, employing Kalman filtering and smoothing for the computation of session-wise coordinates of 104 VLBI radio telescopes over more than 30 years. We compare our VLBI TRF to the multi-technique ITRF solutions ITRF2014 and JTRF2014, focusing on the different approaches of modeling non-linear signals. Overall, a good agreement is found for strong post-seismic deformations, but the three solutions diverge in terms of seasonal signals.

Keywords VLBI, Kalman filter, terrestrial reference frames, post-seismic deformations

1 Introduction

Terrestrial reference frames (TRFs) are important for several applications, for example in the fields of navigation, geophysics, and climate investigations. Therefore, determining TRFs with utmost accuracy and stability is one of the primary tasks of geodesy. In previous generations of International Terrestrial Reference Frame (ITRF) solutions, such as the ITRF2008 [1], the station coordinate model for every segment consisted of an offset and a velocity. In order to take into account non-linear effects and thus satisfy growing accuracy demands, the ITRS (International Terrestrial Reference System) combination centers of the IERS (International Earth Rotation and Reference Systems Service) followed different strategies to extend the coordinate model for the most recent ITRF solutions, comprising data until the end of 2014. For example, all Combination Centers decided to estimate seasonal signals. The two ITRF solutions considered in this study, the ITRF2014[1] by IGN and the JTRF2014 by JPL are discussed in greater detail in Section 3.

At GFZ Potsdam, we have calculated TRF solutions solely based on the data from very long baseline interferometry (VLBI, [2, 3]). VLBI is very important for the determination of TRFs since it is very sensitive to the network scale. Similar to the ITRF solution by JPL, our approach is based on Kalman filtering. More details are provided in Section 2 as well as in Soja et al. (2016) [4].

The aim of this study is to compare these three TRF solutions. In particular, it is of interest how strong non-linear effects, such as post-seismic deformations and seasonal signals, are handled. Therefore, the comparisons of this preliminary study are restricted to stations that are strongly affected by these phenomena.

1. GFZ German Research Centre for Geosciences, Potsdam, Germany
2. Technische Universität Berlin, Berlin, Germany
3. Jet Propulsion Laboratory, California Institute of Technology, Pasadena, United States of America

[1] `http://itrf.ign.fr/ITRF_solutions/2014/`

2 Kalman Filter VLBI TRF Solution

The Kalman filter VLBI TRF solution (from here on KF VTRF) produced at GFZ is based on 4,239 VLBI sessions between 1980 and the end of 2013. Only sessions with four or more radio telescopes participating and with the volume of the polyhedron defined by the network exceeding more than 10^{15} m^3 were considered to ensure that the network geometry is suitable for TRF determination. In the future, it would be worthwhile to consider the inclusion of regional sessions in order to increase the temporal resolution. As input data the session-wise coordinates computed with the VieVS@GFZ software [5, 6], a fork from the Vienna VLBI Software [7], were used. In total, the coordinates of 104 radio telescopes were processed.

For this study, the standard solution portrayed in [4] was used. The state vector of the Kalman filter comprised offsets and velocities of all considered stations. The coordinate offsets were modeled as random walk processes, with the station-specific process noise derived from time series of the geophysical loading effects that were not corrected for in the VLBI analysis, namely non-tidal atmosphere, non-tidal ocean, and continental water storage loading displacements [8]. In order to increase the short-term stability of the frame, the coordinate noise model was scaled by a factor of 0.1. No seasonal signals were estimated, since it was shown [4] that in the presence of process noise, the resulting time series are identical. In order to take into account the non-linear deformations after strong earthquakes, the noise directly after such an event was increased by a factor of 10 for coordinate jumps of 3 m (and scaled linearly for different sizes of jumps). This scaling factor was steadily reduced to the original noise level over a time span of one year.

3 ITRF2014 and JTRF2014

Both ITRF2014 and JTRF2014 are based on the combined SINEX files submitted by the combination centers of the International Association of Geodesy services of the four primary space-geodetic techniques. For both TRFs, the combination was performed on the parameter level, which means that the datum-free normal equations of the VLBI contribution had to be inverted beforehand. Both solutions include annual and semi-annual signals and inferred the scale information from the average of the VLBI and satellite laser ranging scales (weighted in the case of JTRF2014).

The selection of data was significantly different between these two solutions. While for ITRF2014 an extensive set of stations was used, a large portion was eliminated for JTRF2014. For example, in the case of VLBI only 71 stations were used (ITRF2014: 140). Regional sessions were excluded for JTRF2014, similar to the KF VTRF solution. On the other hand, the ITRF2014 creators were selective regarding the local ties, while a comprehensive set of 234 tie vectors, properly weighted by their co-variances, was adopted for JTRF2014.

Still, the main difference lies in the fact that ITRF2014 was computed by least-squares adjusting the parameters of the coordinate model (which also includes exponential and/or logarithmic functions for post-seismic deformations), whereas a Kalman filter and smoother was used for JTRF2014. In the latter, the solution is represented by a time series of weekly station coordinates. Similar to the KF VTRF, the coordinates are modeled as random walk processes with the noise derived from geophysical loading models [9].

4 Comparison of TRF Solutions

As the input data sets are different, even between the two multi-technique solutions due to the heavy data screening and editing, it is difficult to select a reference. Consequently, the comparisons have been kept on a qualitative and visual level. The station coordinates in all graphs are shown in local topocentric coordinate systems, with no trends or other functions subtracted, and thus reflect only the differences between the solutions.

In Figure 1, all three TRF solutions are plotted for station Tsukuba, Japan. Clearly visible is the large displacement and strong post-seismic deformation due to the 2011 Tōhoku earthquake, which all solutions are able to account for. Figure 2 portrays the temporal changes in the east coordinate component after the earthquake in greater detail. It becomes evident that the agreement of these current solutions with the observations is much better than what would be possible with the classical linear model. Nevertheless, small discrepancies between the solutions are visible, in particular during the first months of the post-seismic period, where the ITRF2014 disagrees with the two Kalman filter solutions by up to 1.5 cm.

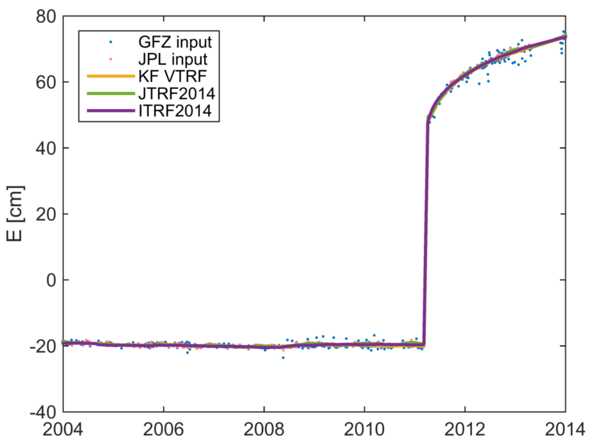

Fig. 1 East coordinates of station Tsukuba from 2004 until 2014 for the KF VTRF solution (yellow), ITRF2014 (green), and ITRF2014 (purple). Additionally, the input coordinates for the VTRF (blue dots) and JTRF2014 (light red dots) are provided.

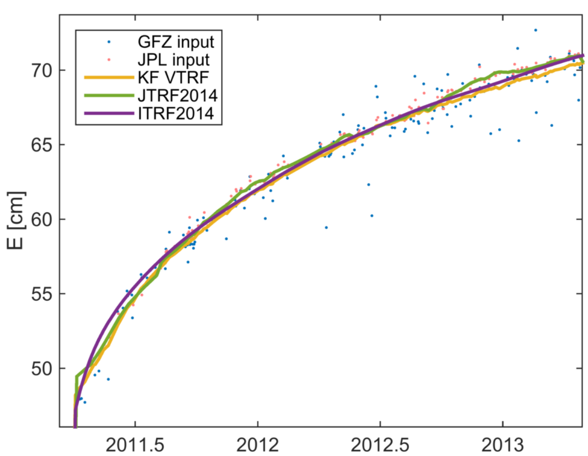

Fig. 2 For the east coordinate of Tsukuba the same data and solutions as in Figure 1 are depicted with a focus on the period after the earthquake.

Figure 3 exhibits the situation of station Tsukuba before the earthquake. Starting from the first half of 2008, a weak seismic signal is visible in all solutions, with coordinates slightly diverging from the long-time trend. The seasonal signals are, however, very different between the three solutions. The annual oscillation

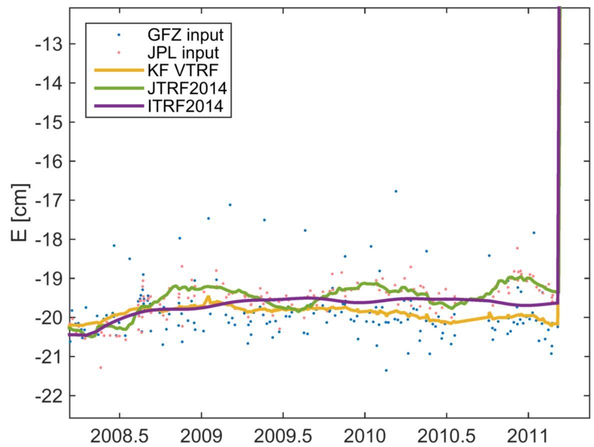

Fig. 3 East coordinates of Tsukuba in the period before the earthquake, otherwise similar to Figure 2.

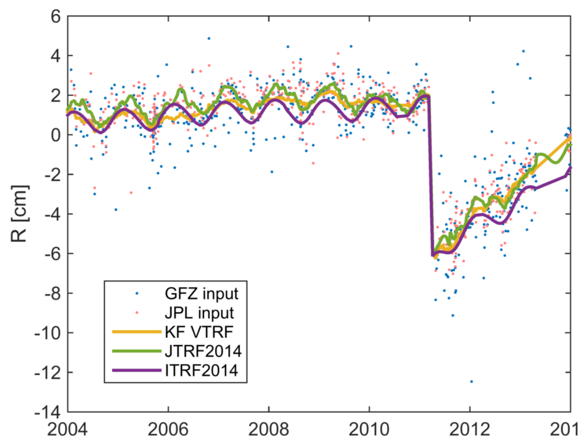

Fig. 4 Height component of Tsukuba between 2004 and 2014 (for details see Figure 1).

in JTRF2014 is significantly larger than in ITRF2014 and seems to be out of phase by about 180°. The phase of the VTRF signals is similar to JTRF2014, but the amplitude fits the one of ITRF2014. A better agreement in terms of seasonal signals is found in the radial component (Figure 4). Here, only the KF VTRF shows smaller amplitudes, however, supported by the input data. In the two multi-technique solutions, a reason for the larger seasonal signals could be co-motion constraints imposed on the co-located GNSS station TSKB, the input data of which shows a distinct annual signal. The trend after the earthquake is different between the Kalman filter solutions and ITRF2014, what is surprising since the agreement is much better in the east component.

In Figure 5, the coordinates of station Gilmore Creek, Alaska, are examined. Similar to the east coordinates of Tsukuba, the three solutions diverge in terms of seasonal signals. Here, the annual signals of irregular amplitudes seen in the two Kalman filter solutions are out of phase. ITRF2014 shows distinct semi-annual signals that are not found in the other solutions. Nevertheless, the seismic effects are well represented in all solutions. A positive effect of the extended coordinate models is that fewer breaks need to be introduced. For example, ITRF2008 introduced six breaks to capture the complex seismic displacements, whereas for the current solutions, it is sufficient to apply just a single break at the epoch of the earthquake.

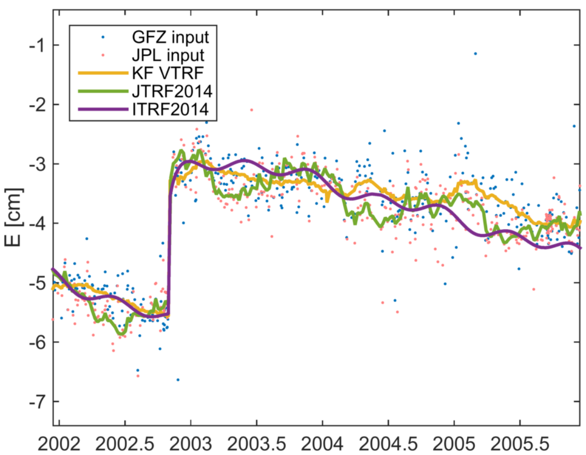

Fig. 5 East coordinates of station Gilmore Creek are shown for the time period 2002–2006. The same TRF solutions as in Figure 1 are included.

Finally, Figure 6 depicts the complex post-seismic behavior of the coordinates of the station in Concepción, Chile, due to the 8.8 M_w earthquake in 2010 and an aftershock in 2011. The JTRF2014 coordinates directly after the earthquake are only based on observations during very few weeks and are therefore mostly predictions, which obviously cannot account for the post-seismic deformations. Once observations are integrated again in mid-2011, JTRF2014 agrees with the other solutions very well. The temporal changes in the coordinates of the KF VTRF and ITRF2014 fit very well over the whole period, although a bias is present.

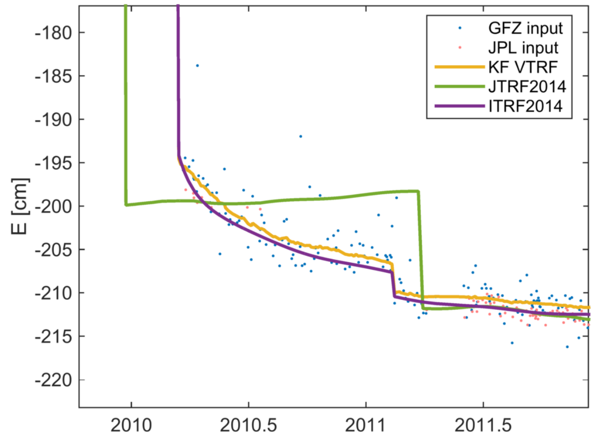

Fig. 6 For station TIGO Concepción, east coordinates during the first years after the 2010 Chile earthquake are given. The same graphical elements as in Figure 1 are shown.

5 Conclusions

In this paper, a VLBI TRF solution based on Kalman filtering and the two International Terrestrial Reference System realizations ITRF2014 and JTRF2014 were compared focusing on non-linear signals. Overall, a good agreement was found during periods of post-seismic deformations. Here, the extension of the coordinate model (in a functional or stochastic sense) allows to closely follow the observed variations, what would not be the case for the classical linear approach. While the seasonal signals from the different solutions are mostly consistent with each other for the height component, striking differences are found in the horizontal components for the considered stations. Considering the different approaches and data sets, the performance of our KF VTRF solution is promising. In the future, the comparisons should be extended to include additional stations as well as the DTRF2014, the ITRF solution by DGFI, Munich.

Acknowledgements

The authors thank the IVS for observing, correlating, and providing the VLBI data used in this work and the ITRS Combination Centers of the IERS at IGN and JPL for providing ITRF solutions. Benedikt Soja works under FWF project P 24187-N21. The work of RG described in this paper was carried out at the Jet Propulsion Laboratory, California Institute of Technology, under a contract with the National Aeronautics and Space Administration.

References

1. Z. Altamimi, X. Collilieux, and L. Métivier. ITRF2008: an improved solution of the international terrestrial reference frame. *Journal of Geodesy*, 85(8):457–473, 2011.
2. H. Schuh and D. Behrend. VLBI: A fascinating technique for geodesy and astrometry. *J. Geodyn.*, 61:68–80, 2012.
3. A. Nothnagel, International VLBI Service for Geodesy and Astrometry (IVS), et al. The IVS data input to ITRF2014. International VLBI Service for Geodesy and Astrometry, GFZ Data Services, DOI 10.5880/GFZ.1.1.2015.002, 2015.
4. B. Soja, T. Nilsson, K. Balidakis, S. Glaser, R. Heinkelmann, and H. Schuh. Determination of a Terrestrial Reference Frame via Kalman Filtering of Very Long Baseline Interferometry Data. *Journal of Geodesy*, submitted.
5. T. Nilsson, B. Soja, M. Karbon, R. Heinkelmann, and H. Schuh. Application of Kalman filtering in VLBI data analysis. *Earth, Planets and Space*, 67(1):136, 2015.
6. B. Soja, T. Nilsson, M. Karbon, F. Zus, G. Dick, Z. Deng, J. Wickert, R. Heinkelmann, and H. Schuh. Tropospheric delay determination by Kalman filtering VLBI data. *Earth, Planets and Space*, 67(1):144, 2015.
7. J. Böhm, S. Böhm, T. Nilsson, A. Pany, L. Plank, H. Spicakova, K. Teke, and H. Schuh. The new Vienna VLBI Software VieVS. In S. Kenyon, M. C. Pacino, and U. Marti, editors, *Proceedings of IAG Scientific Assembly 2009*, volume 136 of *International Association of Geodesy Symposia*, pages 1007–1011. Springer-Verlag, Berlin Heidelberg, 2012.
8. IERS Conventions. G. Petit and B. Luzum (eds.). IERS Technical Note 36, Frankfurt am Main: Verlag des Bundesamtes für Kartographie und Geodäsie, 2010.
9. X. Wu, C. Abbondanza, Z. Altamimi, T. M. Chin, X. Collilieux, R. S. Gross, M. B. Heflin, Y. Jiang, and J. W. Parker. KALREF – A Kalman filter and time series approach to the International Terrestrial Reference Frame realization. *Journal of Geophysical Research: Solid Earth*, pages 3775–3802, 2015.